**Research Article**

# Osteogenic Differentiation and Mineralization on Compact Multilayer nHA-PCL Electrospun Scaffolds in a Perfusion Bioreactor

**Maliheh Yaghoobi [1], Sameereh Hashemi-Najafabadi [1*], Masoud Soleimani [2], Ebrahim Vasheghani-Farahani [1], Seyyed Mohammad Mousavi [3]**

[1]Biomedical Engineering Group, Faculty of Chemical Engineering, Tarbiat Modares University, Tehran, Iran
[2]Hematology Group, Faculty of Medical Sciences, Tarbiat Modares University, Tehran, Iran
[3]Biotechnology Group, Faculty of Chemical Engineering, Tarbiat Modares University, Tehran, Iran

[*]*Corresponding author*: Sameereh Hashemi-Najafabadi, Biomedical Engineering Group, Faculty of Chemical Engineering, Tarbiat Modares University, Tehran, Iran. Tel: +98-2182884384, Fax: +98-2182884931, E-mail: s.hashemi@modares.ac.ir

**Received:** October 28, 2015; **Revised:** January 19, 2016; **Accepted:** February 15, 2016

**Background:** Monolayer electrospun scaffolds have already been used in bone tissue engineering due to their high surface-to-volume ratio, interconnectivity, similarity to natural bone extracellular matrix (ECM), and simple production.
**Objectives:** The aim of this study was to evaluate the dynamic culture effect on osteogenic differentiation and mineralizationi into a compact cellular multilayer nHA-PCL electrospun construct. The dynamic culture was compared with static culture.
**Materials and Methods:** The calcium content, alkaline phosphatase (ALP) activity and cell viability were investigated on days 3 and 7.
**Results:** When the dynamic culture compared to static culture, the mineralization and ALP activity were increased in dynamic culture. After 7 days, calcium contents were 41.24 and 20.44 $\mu g.(cm^3)^{-1}$, and also normalized ALP activity were 0.32 and 0.19 $U.mg^{-1}$ in dynamic and static culture, respectively. Despite decreasing the cell viability until day 7, the scanning electron microscopy (SEM) results showed that, due to higher mineralization, a larger area of the construct was covered with calcium deposition in dynamic culture.
**Conclusions:** The dynamic flow could improve ALP activity and mineralization into the compact cellular multilayer construct cultured in the perfusion bioreactor after 7 days. Fluid flow of media helped to facilitate the nutrients transportation into the construct and created uniform cellular construct with high mineralization. This construct can be applied for bone tissue engineering.

*Keywords*: Mineralization; Electrospun scaffolds; Multilayer construct; Osteogenic differentiation; Perfusion bioreactor

## 1. Background

Bone defects result in significant clinical problems, and hence require sufficient effort to search for bone substitutes for clinical applications. There are several limitations, such as shortage in donor organs, and also host immune responses in bone transplantation. To overcome these obstacles, bone tissue engineering using scaffolds and stem cells have become an attractive subject of research in the past few years. Engineering of these cellular constructs may form a suitable alternative in bone regeneration therapies (1-3).

Stem cells are very attractive for cell-based therapies owing to their self-renewal capacity and differentiation potential (4). Adipose-derived stem cells (ASCs) are multipotent progenitor cells. ASCs can differentiate into many types of cells (5). Due to osteogenic differentiation, human ASCs (hASCs) can be used as a promising cell source for bone regeneration (6).

The electrospinning technique has been used to produce three-dimensional (3D) scaffolds, mimicking the natural extracellular matrix (ECM) structure. It is a simple and versatile method that can fabricate porous nanofibrous structures with large surface-to-volume ratio, interconnected pores and high porosity (7-9). Briefly, a basic electrospinning system usually consists of three major parts: a high voltage power supply, a spinneret, and a grounded collector (usually a metal screen, plate, or rotating mandrel). This process using an electrical field produces non-woven fibers between

nanometer and micrometer sizes in diameter (10-12). Electrospun nanofibrous scaffolds can enhance cell proliferation, osteogenic differentiation, and mineralization (13).

A wide range of natural and synthetic polymers has been applied for electrospinning in bone tissue engineering (14). The chemical structure of natural bone is mainly composed of hydroxyapatite [$Ca_{10}(PO_4)_6(OH)_2$] nanocrystals (nHA) and type I collagen fibrils (15, 16). Generally, nHA as an important component has been used in combination with several polymers, such as poly (ε-caprolactane) (PCL), PCL.collagen$^{-1}$ (Col), PCL.gelatin$^{-1}$ (Gel), poly-L-lactic acid (PLLA).Col$^{-1}$, and poly (3-hydroxy-butyrate-co-3-hydroxyvalerate (PHBV) to prepare the biomimetic nanofibrous scaffolds for bone tissue engineering. Because of its osteoconductive and osteoinductive properties of nHA (17), it can induce secretion of the ECM in cells cultured on the scaffolds containing nHA (18).

The electrospun scaffolds have been used for bone tissue engineering, but a single layer of electrospun scaffold is not sufficient for deep bone defects. This problem can be addressed by replacing the multilayer scaffolds. Static culture of cells on these multilayered scaffolds cannot provide sufficient cells. Hence, dynamic culture of cells on these compressed structures seems to be necessary; to better enhance cell proliferation. Perfusion bioreactor systems can be applied to improve the culture media circulation and convective transport of nutrients to the cells, as well as to produce more uniform tissues (19).

Both monolayer and multilayer electrospun scaffolds have been used for bone tissue engineering. For instance,in a PluriXTM plug-flow bioreactor densely-stacked layers that later used for subcutaneous mice implantation, 30 individual PCL nanofibrous scaffolds containing human stem cells, were incubated for 6 weeks and no compression between layers were noted (20). In another study, the stacked multiple layers of electrospun polydioxanone (PDO)-nHA were used to evaluate the mineralization with simulated body fluid (SBF) (21). Nevertheless, the osteogenic differentiation and mineralization in compact cellular constructs have not been studied in the bioreactors. Bioreactors provide efficient exchange of nutrients and produce homogenous cellular constructs under dynamic medium flow (22).

Here and for the first, hASCs were cultured on a compact multilayer construct of nHA-PCL electrospun scaffolds with an average fiber diameter of 350 nm. The culture was incubated in perfusion bioreactor. The dynamic result was compared with static samples on day 3 and day 7. It was hypothesized that pressing the scaffolds and dynamic culture have profound effects in promoting osteogenic differentiation and mineralization.

## 2. Objectives

The aim of this study was evaluation of the effect of fluid flow in osteogenic differentiation into the compact multilayered electrospun scaffolds. The five layers of nHA-PCL electrospun scaffolds used into the perfusion bioreactors. The result of dynamic culture compared with static culture.

## 3. Materials and Methods

### *3.1. Preparation of Electrospun Scaffolds*

PCL (80 kD) (Sigma-Aldrich), nHA (<200 nm) (Sigma-Aldrich), 99.5% N,N-dimethylformamide (DMF) (Merck, Germany), and chloroform (Merck, Germany) were used. Fabrication of nHA-PCL electrospun scaffolds was previously optimized (23). Briefly, 0.082 g nHA was dispersed in 10 mL chloroform/DMF (85/15 v/v) and sonicated for 15 min at 22ºC. Chloroform/DMF/nHA dispersion was added to 1.5 g PCL and mixed using magnetic stirrer for 2 h. The suspension was sonicated for 15 min to disperse the nanoparticles in the polymer solution.

PCL/nHA scaffolds were produced using an electrospinning machine (Nano spinner TM, Iran). Two syringes containing PCL/nHA suspension were fixed vertically into a syringe pump at 20 cm distance from the collector (aluminum rotating cylindrical drum). Random fibers were prepared in 22 kV applied voltage, 0.5 mL.h$^{-1}$ solution output rate, 600 rpm collector speed, and 45° spray angle. The fabricated scaffolds (100-120 µm in thickness) were treated with oxygen gas plasma at 0.4 mbar pressure for 5 min (Diener Electronics, Germany) to improve the surface hydrophilicity.

### *3.2. Porosity and Pore Size*

Various methods are being used to measure the porosity and pore size of scaffolds. The total porosity (Φ) of scaffolds is measured according to Eq. 1 (24):

$$\Phi=1-\rho_s/\rho_t \quad (1)$$

Where $\rho_s$ is the ratio of scaffold mass to its volume and $\rho_t$ is total density of the components that contribute to fabricate the scaffold.

Scanning electron microscopy (SEM) images were analyzed using Image J software to measure the pore sizes. Sixty pores were randomly selected from three different images with the same magnification to measure the pore size.

*3.3. Cell Culture and Seeding on the Scaffolds*

hASCs were obtained commercially (Stem Cell Technology Research Center, Iran). hASCs were cultured in low-glucose Dulbecco's modified Eagle's medium (DMEM)-Glutamax (GIBCO) containing 10% fetal bovine serum (FBS) (GIBCO), 100 $U.mL^{-1}$ penicillin (GIBCO), and 100 $\mu g.mL^{-1}$ streptomycin (GIBCO) (referred as DM10 medium). hASCs at passage 4 were used. The osteogenic medium containing 0.1 µM dexamethasone (Sigma-Aldrich, USA), 10 mM b-glycerophosphate (Sigma-Aldrich, USA), and 50 µM ascorbic acid 2-phosphate (Sigma-Aldrich, USA) were used for the differentiation. The fabricated nHA/PCL scaffolds were cut into circular disks (10 mm in diameter) and sterilized by immersion in 70% filtered ethanol for 24 h. The disks were rinsed twice with phosphate buffer saline (PBS) for 2 h, and were soaked in DM10 medium for 15 min in 48-well plates. The sterilized scaffolds were seeded with hASCs (15000 cells/ scaffold) and incubated under 5% $CO_2$ for 3 h to attach cells on the plasma treated side. DM10 medium up to 500 µL was slowly added to each well. The seeded scaffolds were transferred to a humidified incubator (37°C and 5% $CO_2$) for 3 days to allow for cell attachment to the scaffolds.

*3.4. Construction of the Perfusion Bioreactor*

The designed perfusion bioreactor system is shown in (Figure 1). Each bioreactor was comprised of two glass cylindrical chambers. The inner diameters of lower and upper chambers were 1.15 and 1.05 cm, respectively. In building the bioreactor and in addition to the glass cylindrical chambers, 2 stainless steel mesh supports to fix the scaffolds, a Teflon cylindrical holder for placing under the scaffolds, two silicon O-rings for sealing, and a Teflon cylindrical piece for interconnecting the glass chambers were used. After sterilizing the system inside the autoclave, the cellular construct (containing 5 layers of scaffold) was placed between two stainless steel mesh supports. The scaffolds were compressed to half of their thickness because the upper cylindrical chamber was placed into the lower chamber, and was twisted with PTFE piece screw-like for sealing the bioreactor. The culture medium was then pumped from the reservoirs into the bioreactors, and returned to the reservoirs by using a multichannel peristaltic pump (Heidolph, Germany) at a flow rate of 4.5 $mL.min^{-1}$. The medium was changed every 2-3 days. The constructs (compact stacked scaffolds) were harvested after 3 and 7 days for cell viability, alkaline phosphatase (ALP) activity, calcium content assay, and scanning electron microscopy (SEM). For static samples, 5 layers of the cellular scaffolds that cultured in 48 wells plate were harvested on day 3 and day 7 for estimation of ALP activity, calcium content and cell viability.

*3.5. MTT Assay*

The viability of cultured hASCs on nHA/PCL scaffolds in the bioreactor was determined using MTT (3-{4,5-dimethylthiazol-2yl}-2,5-diphenyl-2H-tetrazoliumbromide, Atocel, Austria) assay. After rinsing the cellular scaffolds with serum-free medium, 50 µL of MTT solution (5 $mg.mL^{-1}$) was diluted 1:10 with

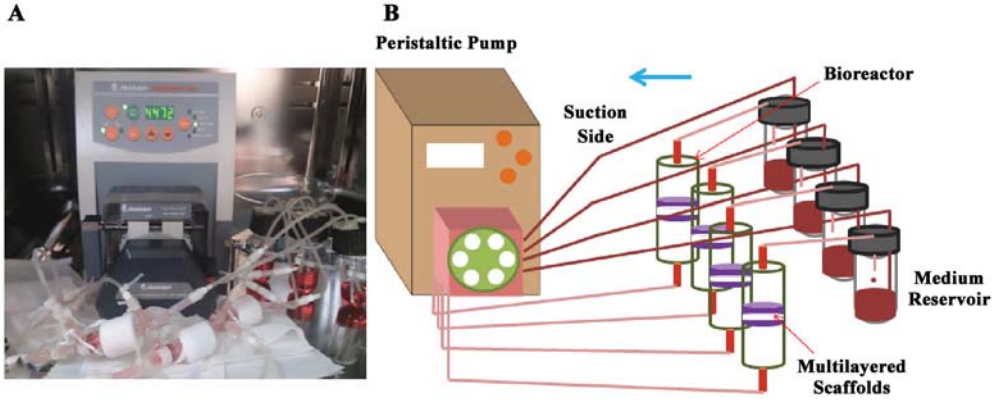


**Figure 1.** A: Direct perfusion bioreactors system, B: The schematic structure of bioreactor system in details

DMEM and added to each well of 48-well plates. Insoluble purple formazan granules were formed following the incubation at humidified incubator (37°C and 5% $CO_2$) for 4 h. Subsequently, the medium was removed, and the purple formazan was dissolved in DMSO (500 mL.well$^{-1}$), and the absorbance of the resulting solution was measured using an automatic microplate reader (ELX 800, Bio-Tek) at 570 nm.

*3.6. ALP Activity*

The level of ALP activities of hASC cultured under static and dynamic cultures were determined after 3 and 7 days (n = 3). The cellular scaffolds were rinsed with PBS, and the cell lysates were extracted using cell lysis buffer containing protease inhibitor cocktail, followed by centrifugation. Cell lysates (50 µL) were mixed with 100 µL pNPP (1 mg.mL$^{-1}$), in 1 M diethanolamine buffer containing $MgCl_2$ (0.5 mM, pH 9.8). The absorbance of the prepared solution was measured at 405 nm following incubation at 37°C for 30 min. Total protein content was determined using BCA protein assay Kit (Thermo Scientific, USA), and the ALP activities were normalized to the total protein content.

*3.7. Calcium Deposition Assay*

Calcium content of the constructs in bioreactors and scaffolds in 48 wells plate (static samples) was quantified using cresolphthalein complexone (CPC) Kit (Pars Azmoon, Iran). Briefly, the constructs were washed with calcium-free PBS, and 1 mL of 0.6 N hydrochloric acid (HCl) added to the constructs for calcium extraction. The samples were shaken at 250 rpm for 1 h. Finally, 20 µL of the solution was mixed with 1 mL solution containing 0.06 mM 2-CPC, 7 mM 8-hydroxyquinoline, detergents, 0.8 M ethanolamine (pH 10.7), and 20 mM HCl (pH 1.1). The absorbance of the final solution was measured at 540 nm in a spectrophotometer (Agilent Technology, USA) followed by incubation at 37°C for 30 min. The calcium content of scaffolds (relating to nHA) before cell seeding was measured and subtracted from the calcium content results.

*3.8. Scanning Electron Microscopy* (*SEM*)

The deposited calcium onto cellular scaffolds was observed using a scanning electronic microscope (Hitachi, Japan). The constructs were rinsed two times with calcium-free PBS and fixed with 2.5% glutaraldehyde at 4°C for 1 h. The samples were dehydrated by ethanol in an increasing concentration gradient (50, 70, 80, 90, and 100%). The layers of construct were separated from each other following drying. The prepared samples were coated with a thin layer of gold for SEM observation.

*3.9. Statistical Analysis*

The obtained data were analyzed using Student's t-test, and the significant level was set at minimum P-value < 0.05. The results were expressed as mean ± SD, n = 3.

## 4. Results

*4.1. Scaffold Characterization and SEM Analysis*

Before cell seeding, the structure of scaffold was evaluated by measuring the pore size, porosity, and mechanical properties. For measuring of porosity, the scaffolds were cut into circles and 20 samples were selected for density ($\rho_s$) measurment. Equation 1 was used to calculate the total porosity. The average porosity was 76.6±2.39% and the average pore size of 60 selected pores from three SEM images was 15.77±1.53 µm. The mechanical properties of the used nHA-PCL electrospun scaffolds optimized by Doustgani *et al.* (23) had strength and module values of 5.4±0.1 and 12.4±0.22 MPa, respectively.

As shown in (Figure 2), calcium deposition was observed in multilayer cellular scaffolds cultured in dynamic and static conditions (Figure 2A-F), even in the middle layers after 7 days (Figure 2A,B). Still, there were a lot of spaces without mineralization in different parts of the cellular scaffolds cultured freely in 48-well plates (monolayer in static condition) (Figure 2E,F). While the cells were directly exposed to nutrients and oxygen, mineralization was low on the surface of the scaffolds. In the perfusion bioreactor, the cellular scaffolds had a compact structure, and majority of the scaffolds' surfaces were covered with the mineralized matrix (Figure 2A-D and G,H). In comparison to the static state, more ECM was observed in dynamic culture. The surface of middle scaffolds was completely covered with the mineralized matrix (Figure 2A-D).

*4.2. Cell Viability*

The cell viability results of static and dynamic cultures are presented in Figure 3. The low and high cell viabilities were observed in dynamic and static cultures, respectively. The optical density of dynamic samples was slightly increased over time up to day 7. The cell viability of static samples was noticeably

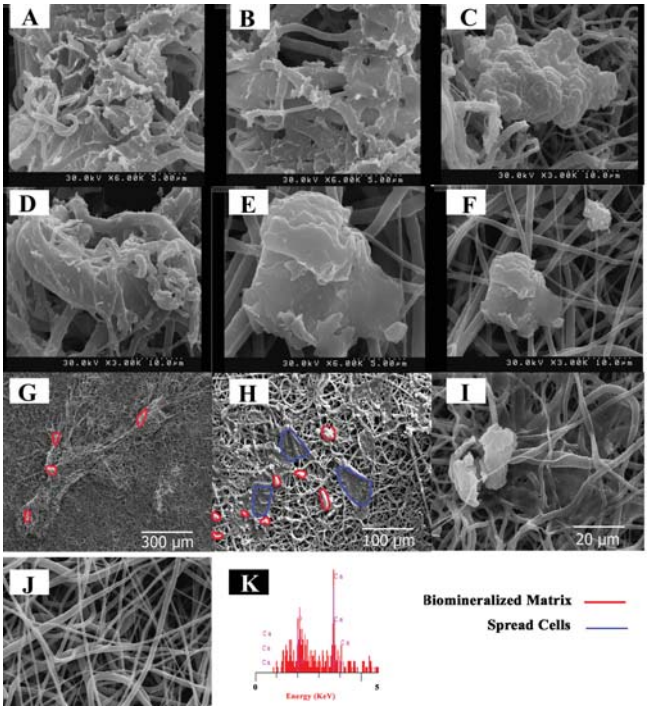


**Figure 2.** SEM images from the cellular scaffolds for calcium deposition after 7 days culture, A, B: The middle layers of the construct in dynamic culture; C, D: The layers were directly exposed to the dynamic culture medium (upper and lower layers of the construct); E, F: Static culture of the monolayer cellular scaffolds; G: Upper layer of the construct in large scale; H: Upper layer of the construct in large scale; I: Static culture of the monolayer cellular scaffolds in large scale; J: The electrospun scaffold before seeding; K: Energy-dispersive X-ray (EDX) from sample A

risen (P-value < 0.05). There was a significant difference between static and dynamic cultures over time (P-value < 0.05).

*4.3. Calcium Deposition on the Filaments of Scaffold*

The mineralized matrix deposition was determined after 3 and 7 days. Figure 4 shows that calcium content of the dynamic and static cultures were increased during the culture time course. When compared to the dynamic culture condition, the calcium deposition in compact stacked scaffolds was higher than that of the cellular scaffolds at static condition. Additionally, as a result of the lower P-values (< 0.05), there was significant differences between two groups.

*4.4. ALP Activity of hASCs in Static and Dynamic Culture*

ALP activity is an early marker of osteoblastic differentiation (25-26). ALP activity was determined after 3 and 7 days, and it was normalized to total protein content per sample (Figure 5). ALP activity of the dynamic culture clearly increased during the culture time (P-value < 0.007). Furthermore, ALP activity of the static culture inclined insignificantly from day 3 to 7. Additionally, after 3 and 7 days, the ALP activity observed in the dynamic culture was clearly greater than that of the static culture.

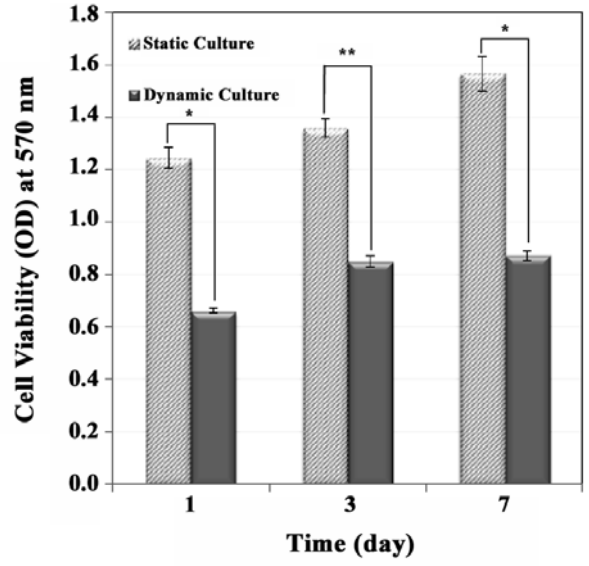


**Figure 3.** The effect of dynamic culture (on a compact construct) in the perfusion bioreactor and static culture on cell viability. The higher cell viability was observed in static culture (only one layer) condition compared with dynamic culture condition (significant difference, P-value * < 0.002 and P-value ** < 0.001)

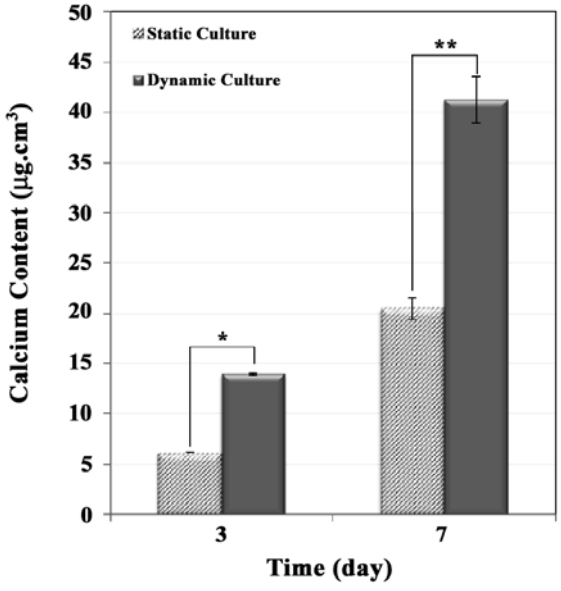


**Figure 4.** Calcium content of a compact construct in the perfusion bioreactor, compared with the static culture (significant difference, P-value * < 0.02 and P-value ** < 0.03)

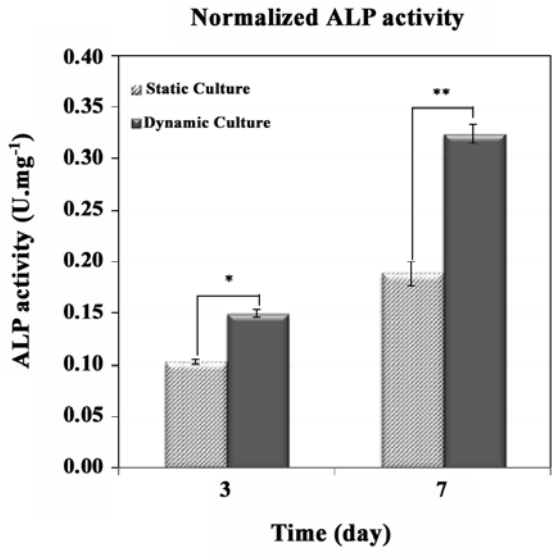


**Figure 5.** ALP activity of a compact cellular construct in the perfusion bioreactor compared with the static culture (significant difference, P-value * < 0.04 and P-value ** < 0.007)

## 5. Discussion

Electrospun scaffolds for bone tissue engineering have attracted the attention of people in recent years. Bone tissue scaffolds require a 3D structure with desirable mechanical properties and great thickness for bone regeneration (27). Electrospun nanofibrous scaffolds are very thin layers (two-dimensional nonwoven) (28, 29), which limits their application in bone tissue engineering. But, preparation of multilayered structure with uniform cell distribution can be efficient in bone tissue engineering. Few studies have been examined the multilayered electrospun scaffolds in dynamic culture condition for bone tissue engineering. For instance, in a study conducted by Srouji (20), the layers were densely stacked into a PluriXTM plug-flow bioreactor, without any mechanical pressure. By contrast, in the present study, an innovative approach has been proposed for cell development on the electrospun scaffolds in a novel type of perfusion bioreactor. Calcification of the construct and ALP activity of the cells were investigated *in vitro* on the compact cellular electrospun scaffolds in a perfusion bioreactor.

The created mechanical stimulation in perfusion bioreactors plays a significant role in nutrient exchange in the thicker structures. These mechanical forces (local strains and interstitial fluid velocities) (30-31) facilitate cell maturation and osteogenic differentiation (32-33). Uniform cell distribution is yet another advantage of the perfusion bioreactor in comparison with the static culture since the cell culture in static condition creates inhomogeneous cell distribution (34). The obtained results showed that the distribution of cells on the scaffolds in the bioreactor was homogeneous (Figure 6A). This cell distribution was visible because of purple MTT formazan crystals in MTT assay that shows live cells in a construct (35). In current study, formation of uniform purple MTT formazan crystals (uniform color) was observed in construct prepared in dynamic culture, as opposed to static culture with no uniform crystals. The size of the scaffolds for both cell culture conditions was similar. After 10 days (3 days for cell attachment on the scaffolds and 7 days for cell differentiation), scaffolds as a whole were not covered with cells in static culture (Figure 6B). It signifies that after cell seeding on the scaffolds and culturing, migration of the cells in dynamic culture was higher than static culture due to the presence of fluid dynamic in the bioreactor. The images were captured from the upper layer of the construct in the bioreactor (Figure 6A) and the cellular scaffold in 48 wells plate (Figure 6B).

The dynamic culture condition provides an osteogenic simulative environment for nHA-PCL cellular multilayer electrospun scaffolds. A comparison between the SEM images of static and dynamic cultures revealed calcium deposition in the constructs of dynamic culture, covering a large area of the scaffolds. This may be due to the uniform distribution of cells in the dynamic culture on the scaffold surface. The cells migrate during the proliferation *in vitro,* but the presence of fluid flow can affect in the direction of movement and accelerate cells movement. Additionally, the functionality of cells is influenced under shear stress by stimulation in interacellur signaling pathways, may include differentiation (or mineralization) (36). The layers were tightly stuck together, and were not easily

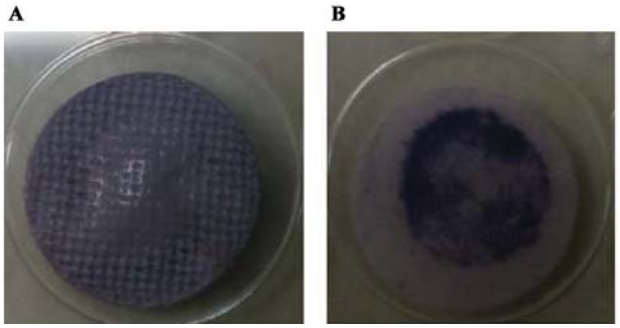


**Figure 6.** The images of purple MTT formazan crystals formation in cellular scaffolds cultured in A: dynamic and B: static culture conditions

separated for SEM analysis after 7 days. During the culture, cells secrete ECM and the layers would be sticky together. At the begining of assembling the bioreactor, the compression increases the attachment of the layers. Moreover the morphology of mineralization is different when the static culture and dynamic culture compared with each other. The layers in the center of the construct were attached to the other layers, but the upper and lower layers of construct were attached from one side. The morphology of calcium deposits was different in central layer from the outer layers. The cellular scaffolds from static culture were freely placed in 48-well plates. In static culture, the cells were spread on the scaffold with low mineralization (Figure 2I).

The flow rate regulation during the osteogenic differentiation was difficult. Since the flow rate was decreased with mineralization of the matrix over time. Therefore, this is one of the challenges that it may occur in perfusion bioreactors for bone tissue engineering. These results demonstrate that the fluid dynamic forces promote the mineralization in a multilayer construct, even with small pore sizes and compact structures.

The results obtained here showed that the newly designed perfusion bioreactor, increases ALP activity and mineralization in the compact nHA-PCL cellular multilayer electrospun scaffolds. In addition, lower number of live cells in dynamic culture condition, as a result of mechanical pressure and fluid dynamic on the cellular construct was noted. Higher ALP activity and mineralization were seen for high cellular monolayer electrospun scaffold cultured in static condition. While the monolayer cellular scaffolds were in direct contact with culture medium in static culture, ALP activity and mineralization was lower than cellular construct in dynamic culture condition.

In some earlier reports, the cell number increases in cellular scaffolds during culturing in the perfusion medium. This increase is mainly dependent on the flow rate of culture medium, and the scaffold type (according to its pore size and porosity) (37). High and low flow rates have also been used for various types of scaffolds and demonstrated that they increase the differentiation and proliferation, respectively (38). The available flow rate of culture medium depends on the scaffold pore size and bioreactor type. Yeatts *et al.* used a tubular perfusion system bioreactor for osteogenic assessment of the suspended cellular nanofibrous scaffolds (39). The flow rate of culture medium was 1 $mL.min^{-1}$. In another study, the flow rate of culture medium was 6.4 $mL.min^{-1}$ in a PluriXTM plug-flow bioreactor (20). In this research, the compact multilayered nHA-PCL scaffolds as a compact construct were placed in the direct perfusion bioreactor for the first time. The flow rate of culture medium was set at 4.5 $mL.min^{-1}$. Furthermore, the mineralized matrix can reduce cellular proliferation (40-41). Therefore, the relatively high flow rate (4.5 $mL.min^{-1}$) could promote osteogenation, but may not lead to cell expansion. Owing to high flow rate, compressed structure and high mineralization not only may inhibit cell expansion but also may decrease cell viability.

## 6. Conclusions

The present study investigated the dynamic culture of seeded hASCs on the nHA-PCL electrospun scaffolds to evaluate the osteogenic differentiation and mineralization. Measurements of ALP activity and calcium content revealed that dynamic culture provides a favorable condition for differentiation of hASCs on compressed cellular electrospun scaffolds. While the exact mechanism of the effect of dynamic culture on osteogenic differentiation remains to be understood, shear stress created by fluid flow can promote osteogenic differentiation of hASCs. Moreover, our results suggested that even with low number of cells, compressing the electrospun scaffolds in the perfusion bioreactor could promote ALP activity and mineralization during the first 7 days. Furthermore, dynamic culture can produce uniform cell distribution in comparison to static culture, which is the great advantage in bone tissue engineering. The development of osteogenic differentiation of hMSCs *in vitro* prior to therapeutic delivery, promote bone repair. Last but not least, due to the successful osteogenic behavior of these scaffolds in dynamic condition, the compressed multilayer scaffolds with uniform cell distribution can provide adequate and effective protection in deep defects.

**Acknowledgments**

This research was supported by Iran National Science Foundation (INSF) under grant No. 92006873 and Tarbiat Modares University, Tehran, Iran.

**References**

1. Eap S, Ferrand A, Palomares CM, Hebraud A, Stoltz JF, Mainard D, et al. Electrospun nanofibrous 3D scaffold for bone tissue engineering. *Biomed Mater Eng*. 2012;**22**(1-3):137-141. DOI: 10.3233/bme-2012-0699

2. Holzwarth JM, Ma PX. Biomimetic nanofibrous scaffolds for bone tissue engineering. *Biomaterials*. 2011;**32**(36):9622-9629. DOI: 10.1016/j.biomaterials.2011.09.009
3. Puppi D, Chiellini F, Piras AM, Chiellini E. Polymeric materials for bone and cartilage repair. *Prog Polym Sci*. 2010;**35**(4):403-440. DOI: 10.1016/j.progpolymsci.2010.01. 006
4. Rodrigues CAV, Fernandes TG, Diogo MM, da Silva CL, Cabral JMS. Stem cell cultivation in bioreators. *Biotechnol Adv*. 2011;**29**(6):815-829. DOI: 10.1016/j.biotechadv.2011.06.009
5. Gimble JM, Katz AJ, Bunnell BA. Adipose-derived stem cells for regenerative medicine. *Circ Res*. 2007;**100**(9):1249-1260. DOI: 10.1161/01.res.0000265074.83288.09
6. Romagnoli C, Brandi ML. Adipose mesenchymal stem cells in the field of bone tissue engineering. *World J Stem Cells*. 2014;**6**(2):144-152. DOI: 10.4252/wjsc.v6.i2.144
7. Ajalloueian F, Tavanai H, Hilborn J, Donzel-Gargand O, et al. Emulsion electrospinning as an approach to fabricate PLGA/Chitosan nanofibers for biomedical applications. *Biomed Res Int*. 2014;**2014**:1-13. DOI: 10.1155/2014/475280
8. Llorens E, Armelin E, Pérez-Madrigal MDM, del Valle LJ, Alemán C, Puiggalí J. Nanomembranes and nanofibers from biodegradable conducting polymers. *Polymers*. 2013;**5**(3):1115-1157. DOI: 10.3390/polym5031115
9. Pillay V, Dott C, Choonara YE, Tyagi C, Tomar L, Kumar P, et al. A Review of the effect of processing variables on the fabrication of electrospun nanofibers for drug delivery applications. *Biomed Res Int.* 2013;**2013**:1-22.DOI:10.1155/2013/789289
10. Demir MM, Yilgor I, Yilgor E, Erman B. Electrospinning of polyurethane fibers. *Polymer*. 2002;**43**(11):3303-3309. DOI:10.1016/S0032-3861(02)00136-2
11. Liang D, Hsiao BS, Chu B. Functional electrospun nanofibrous scaffolds for biomedical applications. *Adv Drug Deliv Rev*. 2007;**59**(14):1392-1412. DOI: 10.1016/j.addr.2007.04.02
12. Yang F, Wolke JGC, Jansen JA. Biomimetic calcium phosphate coating on electrospun poly (ε-caprolactone) scaffolds for bone tissue engineering. *Chem Eng J*. 2008;**137**(1):154-161. DOI:10.1016/j.cej.2007.07.076
13. Bao C, Chen W, Weir MD, Thein-Han W, Xu HHK. Effects of electrospun submicron fibers in calcium phosphate cement scaffold on mechanical properties and osteogenic differentiation of umbilical cord stem cells. *Acta Biomater*. 2011;**7**(11):4037-4044. DOI: 10.1016/j.actbio.2011.06.046
14. Vasita R, Katti DS. Nanofibers and their applications in tissue engineering. Int. *J Nanomedicine*. 2006;**1**(1):15-30
15. Ngiam M, Liao S, Patil AJ, Cheng Z, Chan CK, Ramakrishna S. The fabrication of nano-hydroxyapatite on PLGA and PLGA/collagen nanofibrous composite scaffolds and their effects in osteoblastic behavior for bone tissue engineering. *Bone*. 2009;**45**(1):4-16. DOI: 10.1016/j.bone.2009.03.674
16. Swetha M, Sahithi K, Moorthi A, Srinivasan N, Ramasamy K, Selvamurugan N. Biocomposites containing natural polymers and hydroxyapatite for bone tissue engineering. Int. *J Biol Macromol*. 2010;**47**(1):1-4. DOI: 10.1016/j.ijbiomac.2010.03.015
17. Wang H, Li Y, Zuo Y, Li J, Ma S, Cheng L. Biocompatibility and osteogenesis of biomimetic nano-hydroxyapatite/polyamide composite scaffolds for bone tissue engineering. *Biomaterials*. 2007;**28**(22):3338-3348. DOI: 10.1016/j.biomaterials.2007.04.014
18. Venugopal J, Prabhakaran MP, Zhang Y, Low S, Choon AT, Ramakrishna S. Biomimetic hydroxyapatite-containing composite nanofibrous substrates for bone tissue engineering. *Philos Trans A Math Phys Eng Sci*. 2010;**368**(1917):2065-2081. DOI: 10.1098/rsta.2010.0012
19. Gaspar DA, Gomide V, Monteiro FJ. The role of perfusion bioreactors in bone tissue engineering. *Biomatter*. 2012;**2**(4):167-175. DOI: 10.4161/biom.22170
20. Srouji S, Kizhner T, Suss-Tobi E, Livne E, Zussman E. 3-D Nanofibrous electrospun multilayered construct is an alternative ECM mimicking scaffold. *J Mater Sci Mater Med*. 2008;**19**(3):1249-1255. DOI: 10.1007/s10856-007-3218-z
21. Madurantakam PA, Rodriguez IA, Garg K, McCool JM. Compression of multilayered composite electrospun scaffolds: a novel strategy to rapidly enhance mechanical properties and three dimensionality of bone scaffolds. *Adv Mater Sci Eng*. 2013. DOI: 10.1155/2013/561273
22. Yu P, Lee TS, Zeng Y, Low HT. Fluid dynamics and oxygen transport in a micro-bioreactor with a tissue engineering scaffold. *J Heat Mass Transf*.2009;**52**(1–2):316-327. DOI: 10.1016/j.ijheatmasstransfer.2008.06.021
23. Doustgani A, Vasheghani-Farahani E, Soleimani M, Hashemi-Najafabadi S. Optimizing the mechanical properties of electrospun polycaprolactone and nanohydroxyapatite composite nanofibers. *Compos Part B Eng*. 2012;**43**(4):1830-1836. DOI :10.1016/j.compositesb.2012.01.051
24. Loh QL, Choong C. Three-dimensional scaffolds for tissue engineering applications: role of porosity and pore size. *Tissue Eng Part B Rev*. 2013;**19**(6):485-502. DOI: 10.1089/ten.TEB.2012.0437
25. Owen TA, Aronow M, Shalhoub V, Barone LM, Wilming L, Tassinari MS, et al. Progressive development of the rat osteoblast phenotype *in vitro*: Reciprocal relationships in expression of genes associated with osteoblast proliferation and differentiation during formation of the bone extracellular matrix. *J Cell Physiol*. 1990;**143**(3):420-30. DOI: 10.1002/jcp.1041430304
26. Zur Nieden NI, Kempka G, Ahr HJ. *In vitro* differentiation of embryonic stem cells into mineralized osteoblasts. *Differentiation*. 2003;**71**(1):18-27. DOI: 10.1046/j.1432-0436.2003.700602.x
27. Polo-Corrales L, Latorre-Esteves M, Ramirez-Vick JE. Scaffold design for bone regeneration. *J Nanosci Nanotechnol*. 2014;**14**(1):15-56. DOI: 10.1166/jnn.2014.9127
28. Smith IO, Liu XH, Smith LA, Ma PX. Nano-structured polymer scaffolds for tissue engineering and regenerative medicine. *Wiley Interdiscip Rev Nanomed Nanobiotechnol*. 2009;**1**(2):226-236. DOI: 10.1002/wnan.26
29. Wang X, Ding B, Li B. Biomimetic electrospun nanofibrous structures for tissue engineering. *Mater Today*. 2013;**16**(6):229-241. DOI: 10.1016/j.mattod.2013.06.005
30. Stops AJF, Heraty KB, Browne M, O'Brien FJ, McHugh PE. A prediction of cell differentiation and proliferation within a collagen–glycosaminoglycan scaffold subjected to mechanical strain and perfusive fluid flow. *J Biomech*. 2010;**43**(4):618-626. DOI: 10.1016/j.jbiomech.2009.10.037
31. Yeatts AB, Fisher JP. Bone tissue engineering bioreactors: Dynamic culture and the influence of shear stress. *Bone*.

2011;**48**(2):171-181. DOI: 10.1016/j.bone.2010.09.138
32. Zhang ZY, Teoh SH, Chong WS, Foo TT, Chng YC, Choolani M, et al. A biaxial rotating bioreactor for the culture of fetal mesenchymal stem cells for bone tissue engineering. *Biomaterials*. 2009;**30**(14):2694-2704. DOI: 10.1016/j.biomaterials.2009.01.028
33. Zhang ZY, Teoh SH, Teo EY, Khoon Chong MS, Shin CW, Tien FT, et al. A comparison of bioreactors for culture of fetal mesenchymal stem cells for bone tissue engineering. *Biomaterials*. 2010;**31**(33):8684-8695. DOI: 10.1016/j.biomaterials.2010.07.097
34. Rauh J, Milan F, Gunther KP, Stiehler M. Bioreactor systems for bone tissue engineering. *Tissue Eng Part B Rev*. 2011;**17**(4):263-280. DOI: 10.1089/ten.TEB.2010.0612
35. Ciapetti G, Cenni E, Pratelli L, Pizzoferrato A. *In vitro* evaluation of cell/biomaterial interaction by MTT assay. *Biomaterials* 1993;**14**(5):359-364. DOI: 10.1016/0142-9612(93)90055-7
36. Yourek G, McCormick SM, Mao JJ, Reilly GC. Shear stress induces osteogenic differentiation of human mesenchymal stem cells. *Regen Med*. 2010;**5**(5):713-724. DOI:10.2217/rme.10.60
37. Kim J, Ma T. Perfusion regulation of hMSC microenvironment and osteogenic differentiation in 3D scaffold. *Biotechnol*. Bioeng. 2012;**109**(1):252-261. DOI: Yeatts AB, Both SK, Yang W, Alghamdi
38. Liu M, Liu N, Zang R, Li Y, Yang S-T. Engineering stem cell niches in bioreactors. World J Stem Cells. 2013;**5**(4):124-135. DOI: 10.4252/wjsc.v5.i4.124
39. Yeatts AB, Both SK, Yang W, Alghamdi HS, Yang F, Fisher JP, et al. In vivo bone regeneration using tubular perfusion system bioreactor cultured nanofibrous scaffolds. Tissue Eng Part A. 2014;**20**(1-2):139-146. DOI: 10.1089/ten.tea.2013.0168
40. Chunqiu Z, Xin D, Han W, Weimin Z, Dong Z. Perfusion-compression bioreactor as the optimum choice for growing large-sized engineered bone constructs in vitro. Biosci Hypotheses. 2008;**1**(6):319-323. DOI: 10.1016/j.bihy. 2008.05.008
41. Liao J, Guo X, Nelson D, Kasper FK, Mikos AG. Modulation of osteogenic properties of biodegradable polymer/extracellular matrix composite scaffolds generated with a flow perfusion bioreactor. Acta Biomater. 2010;**6**(7):2386-2393. DOI: 10.1016/j.actbio.2010.01.011